Coupled hydro-mechanical influence on hydraulic conductivity of well-graded sandy gravel

Chenghao Chen [i)], Shiang Mei [ii)], Yi Tang [iii)] and Shengshui Chen [iv)]

i) Ph.D Student, Dept. Geotechnical Engineering, Nanjing Hydraulic Research Institute, 223, Guangzhou Rd., Nanjing 210098, China.
ii) Ph.D Student, Dept. Geotechnical Engineering, Nanjing Hydraulic Research Institute, 223, Guangzhou Rd., Nanjing 210098, China.
iii) Engineer, Dept. Geotechnical Engineering, Nanjing Hydraulic Research Institute, 223, Guangzhou Rd., Nanjing 210098, China.
iv) Professor, Dept. Geotechnical Engineering, Nanjing Hydraulic Research Institute, 223, Guangzhou Rd., Nanjing 210098, China.

ABSTRACT

In embankment dams and hydraulic structures, locally excavated sandy gravel is extensively used as the major rockfill material for its relatively low cost. As an increasing number of hydraulic buildings are designed with higher height and are constructed at steep valleys as well as turbulent waterways, the hydraulic conductivity performance of this building material becomes a vital parameter to evaluate the structure safety against seepage. This paper focuses on the changes of hydraulic conductivity induced by coupling effect of hydraulic load and mechanical behavior. Multi-stage hydraulic heads as well as various stress states are achieved by a newly developed apparatus to replicate infield sophisticated conditions. Sufficient specimen size is provided so that the well-graded test soil remains its natural gradation during constant water head permeability tests. The outflow of soil specimen was measured for each test. It is revealed that both the hydraulic and the mechanical effect result in a global decrease of gravelly material. A threshold of more than 6 MPa exists, indicating that the impact of further stress loading remains to a limited extent. In addition, no observation of obvious seepage failure illustrates that both hydraulic and mechanical loads are favorable to seepage prevention and corresponding countermeasures.

Keywords: sandy gravel, hydraulic conductivity, hydro-mechanical coupling, dam safety

1 INTRODUCTION

The study of seepage characteristics of soil is of great importance when selecting dam designs and carrying out safety assessment of hydraulic structures. In most cases, the pivotal function of dam structures remains the fulfilment of retaining upstream water reservoir. In order to meet this requirement and to guarantee a safe operation of the dam, seepage characteristic of dam-building material needs to be carefully investigated.

With dam construction plans increasingly approved and progressed in north-western area of China, undesirable geological conditions of this mountainous area such as steep bank slope and narrow valley demands that dams be of greater height. Some of the dam design height exceeds 300 m and therefore lead to a huge variance between upstream and downstream water level. This unprecedented height creates a brand new research focus where seepage characteristics under the coupling of high stress level and high hydraulic gradient needs further exploration. To the best of author's knowledge, the maximal stress state realized in plain-strain seepage tests achieved 2 MPa (Zou et al., 2013). This stress level is far lower than what could be engendered by 300 m high dam. The commonly remote location of dam site in north-west China also places restrictions on the transportation of high-quality dam-building materials. In other words, locally excavated materials such as wide-graded sandy gravels are intensively utilized as rock-fill material for dam building. These natural soils often fail to conform to the commonly applied in-field control size of 60 mm due to the geological condition of nearby quarries. Previous studies show that wide-graded soil with coarser grain particles not only results in larger permeability of soil, but also influences the capacity against seepage erosion (Dallo et al., 2013; Ricardo et al., 2017; Nguyen et al., 2017). While some seepage experiments with authentic particle size distribution (PSD) were carried out to investigate the seepage characteristic of wide-graded soil, few researchers have implemented investigations with respect to coupled hydro-mechanical influences (Tomlinson and Vaid, 2000; Moffat and Herrera, 2015).

In this paper, a series of equi-compressional triaxial seepage experiments was conducted to investigate the seepage characteristics of well-graded gravelly soil. No replacement of coarse gravel particles ensures that the hydraulic properties of test soil are studied with no discrepancy. Different stress states were achieved and stress level was gradually augmented until reaching the peak stress level of 7.75 MPa which is adequate to represent stress level of 300 m level dam. Hydraulic factors were studied by three levels of high hydraulic gradient.

2 TEST APPARATUS

A newly developed apparatus has been in use to replicate the seepage phenomenon under high stress conditions. As shown in Fig. 1, this three dimensional loading system allows the exertion of forces along frontal sidewall, along right sidewall and bottom sidewall independently. The maximal stress which could be steadily maintained onto the testing chamber achieves 7.75 MPa. High water energy head is realized by the pressure of compressed air inside the pressure tank. The testing chamber holds a specimen of 900 mm long, 450 mm wide and 450 mm high when all force-transmitted moveable panels are compressed to its limitation. As a result, the particle size permitted in this test apparatus can no longer exceeds 1/5 the minimum size of the permeable cell, that is to say 90 mm according to Industry Code of China: Standard for Soil Test Method (GB/T50123-2019). The set of inlet water system, testing chamber and the water outlet makes up for the seepage circulation.

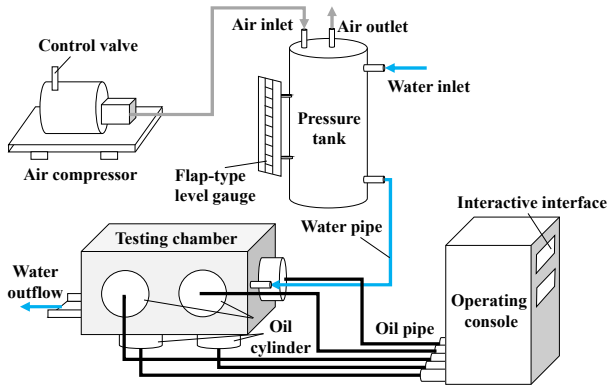

Fig. 1. Schematic of the test apparatus.

3 TRIAXIAL SEEPAGE EXPERIMENTS

3.1 Soil type

The soil intended for this study was sampled from the cladding in Batang Hydropower Station. The sample process was employed on multiple well-distributed excavation sites near the dam. This soil is mainly composed of gravel and sand, with its grain-size distribution curve being presented in Fig. 2.

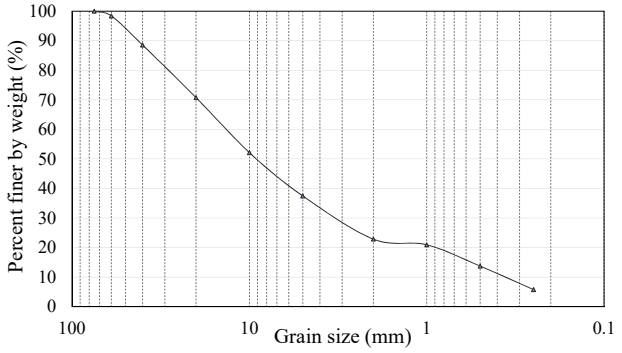

Fig. 2. Particle size distribution of test soil.

The soil is classified as GW according to Standard Practice for Classification of Soils for Engineering Purposes, Unified Soil Classification System (ASTM D2487-17). The index properties are shown in Table 1.

Table 1. Index properties of test soil.

Physical Property	Value
Specific Gravity, G_s	2.78
Dry Density, ρ_d (g/cm^3)	1.92
Percentage of Gravel (%)	62.5
Percentage of Sand (%)	37.5
Mean Particle Size, d_{50} (mm)	9.27
Coefficient of Uniformity, C_u	39.1
Coefficient of Curvature, C_c	2.32

3.2 Specimen preparation

Test soil was installed into the specimen chamber by 3 layers and each time the soil layer of the same thickness was placed and then statically compacted to controlled dry density of 1.92 g/cm^3. Then via the water inlet and the water circulation pipe, water with no hydraulic pressure was supplied into the testing chamber for specimen saturation. The water outlet keeps open until the outflow and inflow reached a balance. Afterwards, both valves of outlet and inlet were shut down and 24 hours were given, allowing the water to completely infiltrate through the porous structure of soil.

After the preparation and saturation of soil specimen, identical compressive pressures along all three directions were exerted onto the testing chamber while other three sidewalls functioned as fixed boundaries. Hydraulic heads were afterwards applied to the specimen when these pressures powered by oil cylinder were stabilized.

4 TEST RESULTS

A series of constant-head permeability tests was conducted under different equi-compressional stress states and various levels of hydraulic heads. Reynolds number is firstly checked by the following equation:

$$\mathrm{Re} = \frac{\rho v d_{10}}{\mu} < 1 \qquad (1)$$

where Re is Reynolds number, ρ is fluid density, v is fluid velocity, d_{10} is particle diameter at 10% finer by weight and μ is fluid dynamic viscosity. Re_{max} in this test equals 0.072, so that flow regime is considered as laminar and Darcy's law is applicable under coupled hydro-mechanical conditions.

Test results presented in Fig. 3 shows the relationship between the hydraulic conductivity and the compressive stress level. Under all hydraulic gradients equaling to 81, 122 and 228, the hydraulic conductivity of test soil decreases with stress level increasing on a global scale. This is because soil is compacted due to high

compressive stress and becomes denser, indicating the diminution of existing pores inside the soil and as a result the decrease of connected pore channels. This downward trend also implies that the phenomenon of internal erosion within test soil is either not triggered or is self-healed. This result fails to support the internal stability criteria (Kenney and Lau, 1985, 1986) or the lately proposed extended internal stability criteria (Chang and Zhang, 2013a). Nevertheless, such controversy could be ascribed to the effect of interlocking induced by high confining stress (Wautier et al., 2019).

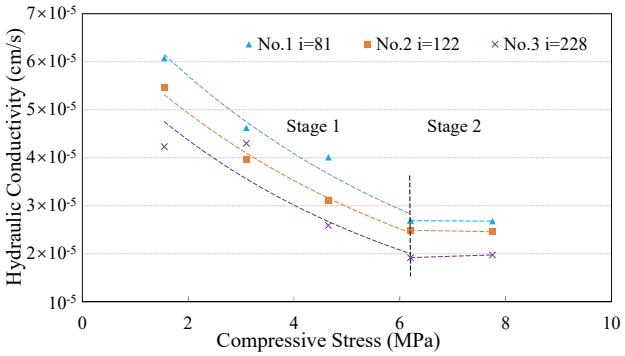

Fig. 3. Relationship between the hydraulic conductivity and equi-compressional stress level.

5 COUPLED HYDRO-MECHANICAL INFLUENCE

The detailed variation of the hydraulic conductivity shares the similar pattern under different high hydraulic gradients. In the first stage, the hydraulic conductivity initially decreases sharply and then the dropping rate turns gradually slow. The relationship between the hydraulic conductivity and the compressive stress could be well described by a series of negative exponential functions which is shown in Table 2. These expressions conform to the estimation formula of hydraulic conductivity with respect to stress (Louis, 1974):

$$k_f = k_0 e^{\alpha\sigma} \tag{2}$$

where k_f is the hydraulic conductivity under different stress, k_0 is the initial hydraulic conductivity equaling to 8×10^{-5}, 7×10^{-5}, 6×10^{-5} cm/s under different hydraulic gradients, α is the coupling parameter and σ is the compressive stress applied to soil specimen.

Table 2. Fitting expression for $k - \sigma_c$ relationship.

Hydraulic Gradient, i (m/m)	Fitting Expression	Correlation Coefficient, R^2
82	$k = 8\times10^{-5} e^{-0.167\sigma_c}$	0.9668
122	$k = 7\times10^{-5} e^{-0.168\sigma_c}$	0.9928
228	$k = 6\times10^{-5} e^{-0.186\sigma_c}$	0.8894

In our case α appears to keep constant while k_0 shows a negative correlation with the level of hydraulic gradient. It is worth noting that the k_0 is comparatively low because of severe hydraulic conditions in which seepage failure of gravelly soil will occur under regular stress state. Therefore k_0 does not fully reflect the hydraulic properties of sandy gravel at initial stage.

When the stress level is higher than a particular number, the downward variation becomes almost neglected. In our case, the threshold stress for all three tests is around 6.2 MPa. In this second stage, it is found that hydraulic conductivities of soil specimen under hydraulic gradient of 81, 122, 228 equal to 2.7×10^{-5}, 2.5×10^{-5}, 1.9×10^{-5} cm/s respectively, displaying a tendency towards stabilization under high stress state and high water head. This could be attributed to the distinguishment of two hypothetical void fractions, namely active voids and inactive voids (Chang et al., 2017). According to the definition, active voids are susceptible to compression and could be thoroughly eliminated due to particle rearrangement, while inactive voids are intrinsic structures of soil and are immune to compressive behavior. These inactive voids which determine the hydraulic conductivity of test soil become more dominant as high stress progressively reduces active voids. Finally, as literally all active voids are removed due to high stress, the volume of void tends to maintain at a certain level and so does the hydraulic conductivity. This interpretation is also supported by numerical simulations of particle mixtures (Wong and Kwan, 2014; El-Husseiny et al., 2019).

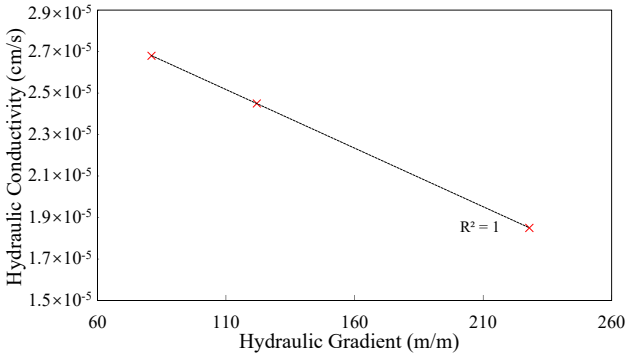

Fig. 4. Relationship between the definitive hydraulic conductivity and hydraulic gradient.

The increase of hydraulic gradient also results in less permeability within test soil. Fig. 4 describes the relationship between definitive hydraulic conductivity and the hydraulic gradient. As the hydraulic gradient increases, the final hydraulic conductivity under high compressive stress state in stage 2 decreases. This negative relationship is perfectly linear in our tests and indicates that the hydraulic gradient is not only a pivotal indicator for seepage failure (Chang and Zhang, 2013b) but also an influence factor when determining the hydraulic conductivity under high stress conditions.

With stress levels rising, the range of hydraulic conductivity is constantly within the same order of magnitude. More specifically, the ratio between k_{max} and

k_{min} (k_{max}/k_{min}) under high hydraulic gradients of 81, 122 and 228 equals to 2.27, 2.22, 2.14, respectively. The influence of hydraulic gradient is similar, as k_{max}/k_{min} under different high stress conditions varies between 1.20 and 1.55. Both factors appear to enhance the soil impermeability and are beneficial to seepage prevention in high dams. Among all hydraulic conductivities in this paper, soil specimen under the least coupled loading condition (1.55 MPa confining stress, hydraulic gradient 81) and that under the second heaviest coupled loading condition (6.2 MPa confining stress, hydraulic gradient 228) have the least and most impermeable properties respectively; the global ratio $(k_{max}/k_{min})_{global}$ is 3.17. Therefore, although further test results are required to validate our findings, special attention should be paid to seepage monitoring results on high dams when the hydraulic conductivity undergoes a severe fluctuation, as factors other than high hydro-mechanical loads are responsible and can be dangerous.

6 CONCLUSIONS

In this paper, a novel seepage apparatus was briefly introduced and a series of seepage tests has been employed by using this apparatus. Wide-graded soil with original maximal grain size reaching 75 mm was used and no replacement of coarse particle was conducted. Multi-stage equi-compressional stress levels were applied to the soil specimen and the hydraulic conductivity under each stage was measured and calculated. Three high hydraulic heads representing multiple hydraulic conditions were replicated to assess the reliability of the test.

Test results reveal a 2-stage evolution of hydraulic conductivity with stress level rising under different gradients. Hydraulic conductivity exhibits a negative exponential function with compressive stress states in the first stage. Soil permeability initially undergoes a fast decrease and then the dropping curve becomes progressively moderate as the stress level increases. In the second stage, soil conductivity becomes stable regardless of the further augmentation of stress levels; this definitive conductivity shows a flawless negative linearity with hydraulic gradient rising. The variation of hydraulic conductivity is restricted to a limited extent under different coupled hydro-mechanical conditions.

ACKNOWLEDGEMENTS

This work was financially supported by the National Key Research and Development Program of China (Grant No. 2017YFC0404805) and the National Natural Science Foundation of China (Grant No. 51539006, 51779153).

REFERENCES

1) ASTM International (2017): Standard Practice for Classification of Soils for Engineering Purposes (Unified Soil Classification System), *ASTM D2487-17*, ASTM International., 1-10. https://doi.org/10.1520/D2487-17
2) Chang, C. S., Meidani, M., and Deng, Y. (2017): A compression model for sand–silt mixtures based on the concept of active and inactive voids, *Acta Geotechnica*, 12(6), 1301–1317. https://doi.org/10.1007/s11440-017-0598-1
3) Chang, D. S., and Zhang, L. M. (2013a): Extended internal stability criteria for soils under seepage. *Soils and Foundations*, 53(4), 569–583. https://doi.org/10.1016/j.sandf. 2013.06.008
4) Chang, D. S., and Zhang, L. M. (2013b): Critical Hydraulic Gradients of Internal Erosion under Complex Stress States, *Journal of Geotechnical and Geoenvironmental Engineering*, 139(9), 1454–1467. https://doi.org/10.1061/(ASCE)GT.1943-5606.0000871
5) Dallo, Y. A. H., Wang, Y., and Ahmed, O. Y. (2013): Assessment of the internal stability of granular soils against suffusion, *European Journal of Environmental and Civil Engineering*, 17(4), 219–230. https://doi.org/10.1080/ 19648189.2013. 770613
6) El-Husseiny, A., Vanorio, T., and Mavko, G. (2019): Predicting porosity of binary mixtures made out of irregular nonspherical particles: Application to natural sediments, *Advanced Powder Technology*, 30(8), 1558–1566. https://doi. org /10.1016/j.apt. 2019.05.001
7) Kenney, T. C., and Lau, D. (1985): Internal stability of granular filters, *Canadian Geotechnical Journal*, 22(2), 215–225. https://doi.org/10.1139/t85-029
8) Kenney, T. C., and Lau, D. (1986): Internal stability of granular filters: Reply, *Canadian Geotechnical Journal*, 23(3), 420–423. https://doi.org/10.1139/t86-068
9) Louis, C. (1974): Rock hydraulics in rock mechanics, New York: Verlag Wien.
10) Ministry of Water Resources of PRC (2019): Standard for Soil Test Method, *GB/T50123-2019*, China Water Power Press Co. Ltd., 330-336 (in Chinese).
11) Moffat, R., and Herrera, P. (2015): Hydromechanical model for internal erosion and its relationship with the stress transmitted by the finer soil fraction, *Acta Geotechnica*, 10(5), 643–650. https://doi.org/10.1007/s11440-014-0326-z
12) Nguyen, C., Benahmed, N., Philippe, P., and Diaz Gonzalez, E. V. (2017): Experimental study of erosion by suffusion at the micro-macro scale, *EPJ Web of Conferences*, 140, 3–6. https://doi.org/10.1051/epjconf/201714009024
13) Ricardo, N. C., Caldeira, L. M. M. S., and Maranha das Neves, E. (2017): Factors limiting the progression of internal erosion in zoned dams: Flow limiting by an upstream material, *Journal of Geotechnical and Geoenvironmental Engineering*, 143(1), 1–10. https://doi.org/10.1061/(ASCE)GT.1943-5606. 0001576
14) Tomlinson, S. S., and Vaid, Y. P. (2000): Seepage forces and confining pressure effects on piping erosion, *Canadian Geotechnical Journal*, 37(1), 1–13. https://doi.org/10.1139/ cgj-37-1-1
15) Wautier, A., Bonelli, S., and Nicot, F. (2019): DEM investigations of internal erosion: Grain transport in the light of micromechanics, *International Journal for Numerical and Analytical Methods in Geomechanics*, 43(1), 339–352. https:// doi.org/10.1002/nag.2866
16) Wong, V., and Kwan, A. K. H. (2014): A 3-parameter model for packing density prediction of ternary mixes of spherical particles, *Powder Technology*, 268, 357–367. https://doi.org/ 10.1016/j.powtec.2014.08.036
17) Zou, Y. H., Chen, Q., and He, C. R. (2013): A new large-scale plane-strain permeameter for gravelly clay soil under stresses, *KSCE Journal of Civil Engineering*, 17(4), 681–690. https:// doi.org/10.1007/s12205-013-0217-0